

Effect of an External Magnetic Field on Some Statistical Properties of the 2+1 Dirac-Moshinsky Oscillator

A. S.-F. Obada¹, M. M. A. Ahmed¹, M. Abu-Shady² and H. F. Habeba²

Department of Mathematics, Faculty of Science, Al-Azher University,
Nassr City 11884, Egypt¹

Department of Mathematics and Computer Science, Faculty of Science,
Menoufia University, Shebin Elkom 32511, Egypt²

Abstract

The 2+1 Dirac-Moshinsky oscillator (2+1 DMO) is mapped into the generalized Jaynes-Cummings model (GJCM), in which an external magnetic field is coupled to an external isospin field. The basic equations of model are analytically solved, where the coherent state is considered as an initial state. The obtained results show that the strength of the magnetic field and the coupling parameter of the isospin field play important roles on some statistical properties such as entanglement, population inversion and degree of coherence. It has been shown that these parameters play a rule to increase entanglement and show the collapses and revivals phenomenon.

Keywords: Dirac-Moshinsky oscillator; generalized Jaynes-Cummings model; Entanglement.

1 Introduction

In quantum optics, the JCM is composed of a single two-level particle interacting with a single quantized cavity mode of the electromagnetic field [1]. This model is exactly solvable in the rotating wave approximation and experimentally realized [2]. It has been found that the JCM has some statistical properties that are not in classical fields, such as the degree of coherence, the collapses and revivals phenomenon and squeezing [3, 4].

JCM has been used to elucidate the strong quantum correlation (entanglement), which is an important aspect of quantum systems. It demonstrates correlations, that cannot be discussed classically [5].

The Dirac oscillator was suggested [6, 7] and reinvestigated where the linear term $im\omega c\beta\alpha.r$ is added to the relativistic momentum of the free-particle Dirac equation [8, 9].

The 1+1 Dirac-Moshinsky oscillator (1+1 DMO) has been exactly solved by using the theory of the non-relativistic harmonic oscillator [10, 11]. The Dirac oscillator has attracted a lot of attention and found many applications in different branches of physics [12–15]. In the other hand the 2+1 dimensions have been related to quantum optics via the JCM [15, 16].

One of the most exciting properties of the DMO is its connection to quantum optics [17, 18]. The connection to the quantum optics allows to conceive quantum optics experiments that emulate this system. The dynamics of the 2+1 DMO were studied [19], in which an exact mapping of this quantum relativistic system into the JCM is obtained. In [20], the 2+1 DMO in the presence of an external magnetic field has been studied. Also, the connection between anti-JCM with the DMO in a magnetic field was established without making any limit on the strength of the magnetic field.

The 1+1 and 2+1 DMO have been mapped to the JCM and the dynamical features of a Dirac particle under the influence of the external field have been studied only at vacuum state [21]. The previous attempts [21] concentrated on the number state without using the coherent state, where the external isospin field is included only, also in Ref. [19] the 2+1 DMO in an external magnetic field has been studied

without any study of statistical properties of the system.

In [22] the 2+1 DMO coupled to an external field has been mapped into the JCM . The effect of both the detuning parameter and the coherence angle on the entanglement and the population inversion have been studied by using two cases for the initial state: the number state and the coherent state. It has been shown that the coherent state gives good description for the entanglement and the population inversion.

In this paper, we study the Dirac oscillator coupled to an isospin field in the presence of an external magnetic field by mapping it to the GJCM. The wave function is obtained by using the coherent state as an initial state. In addition, we study the influence of both the strength of the magnetic field and the coupling parameter of the isospin field on some non-classical properties of the system.

This paper is arranged as follows: Sec. 2 is devoted to introduce basic equations and relations. Sec. 3 is devoted to explain the mapping of 2+1 DMO in an external magnetic field coupled to an external isospin field into the GJCM. Sec. 4 is devoted to the analytical solution of the model, this is followed by a discussion of some non-classical properties in Sec. 5. Finally, in Sec. 6, we conclude this paper with some brief remarks.

2 Basic equations and relations

2.1 The 2+1 Dirac-Moshinsky Oscillator

The DMO is introduced by Moshinsky and Szczepaniak [8] by adding the linear term $im\omega c\beta\alpha.r$ to the Dirac Hamiltonian for a free particle. In the non-relativistic limit, it corresponds to the harmonic oscillator plus a spin-orbit coupling term. The DMO model in 2+1 dimensions takes the following form [21]

$$i\hbar\frac{\partial}{\partial t}|\psi\rangle = \left[\sum_{j=1}^2 c\alpha_j(p_j + im\omega\beta r_j) + mc^2\beta\right]|\psi\rangle, \quad (2.1)$$

where c is the speed of light, m is the rest mass of the particle. α_j and β are the Dirac matrices in the standard representation, they are taken here as $\alpha_1 = -\hat{\sigma}_y$,

$\alpha_2 = -\hat{\sigma}_x$ and $\beta = \hat{\sigma}_z$, where the $\hat{\sigma}$'s are the Pauli matrices. ω represents the harmonic oscillator frequency. We note that the standard Dirac equation is recovered at $\omega = 0$ [23].

The 2+1 DMO in an external magnetic field takes the following form [19]

$$\hat{H}^2 = \sum_{j=1}^2 c\alpha_j(p_j - \frac{e\mathbf{A}_j}{c} - im\omega\beta r_j) + mc^2\beta, \quad (2.2)$$

where e is the charge of the DMO and \mathbf{A} is the vector potential. We take the magnetic field \mathbf{B} in the z -direction, so the vector potential for this particular magnetic field takes the form $\mathbf{A} = (\frac{-B}{2}y, \frac{B}{2}x, 0)$, or $\mathbf{A} = \frac{1}{2}(\mathbf{B} \wedge \mathbf{r})$.

2.2 The generalized Jaynes-Cummings model

We briefly introduce the GJCM, in order to study and connect it with more general and complicated systems, besides the Dirac oscillator.

It is a theoretical model in quantum optics. It describes the system of a two-level particle interacting with one mode of the electromagnetic field without using the rotating wave approximation. The Hamiltonian in the interaction picture takes the following form [24]

$$\hat{H}_{JC} = \Omega(\hat{\sigma}_+ + \hat{\sigma}_-)(\hat{a} + \hat{a}^\dagger) + \delta\hat{\sigma}_z, \quad (2.3)$$

where Ω is the particle-field coupling constant, the operators $\hat{\sigma}_+$ and $\hat{\sigma}_-$ are the raising and lowering operators for the two-level system, they satisfy the commutation relations $[\hat{\sigma}_z, \hat{\sigma}_\pm] = \pm 2\hat{\sigma}_\pm$ and $[\hat{\sigma}_+, \hat{\sigma}_-] = \hat{\sigma}_z$. \hat{a}^\dagger and \hat{a} are the Boson creation and annihilation operator respectively which satisfy the commutation relation $[\hat{a}, \hat{a}^\dagger] = 1$. δ stands for the detuning of the atomic transition frequency from the cavity mode frequency.

3 Mapping of the 2+1 DMO model in an external magnetic field coupled to an external isospin field into the GJCM

By using the spinor $|\psi\rangle = \begin{bmatrix} |\psi_1\rangle \\ |\psi_2\rangle \end{bmatrix}$ and $\hat{H}^2 |\psi\rangle = E |\psi\rangle$, Eq. (2.2) becomes a set of coupled equations as follows

$$(E - mc^2) |\psi_1\rangle = (2cp_z + im\tilde{\omega}\bar{z}) |\psi_2\rangle \quad (3.1)$$

$$(E + mc^2) |\psi_2\rangle = (2cp_{\bar{z}} - im\tilde{\omega}z) |\psi_1\rangle, \quad (3.2)$$

where

$$p_z = \frac{1}{2}[p_x - ip_y], p_{\bar{z}} = \frac{1}{2}[p_x + ip_y], \quad (3.3)$$

$$z = (x + iy), \bar{z} = (x - iy), \quad (3.4)$$

$$\tilde{\omega} = \omega + \frac{\omega_c}{2}, \quad (3.5)$$

with $\omega_c = \frac{|eB|}{mc}$ is the cyclotron frequency.

We can write \hat{H}^2 in the following matrix form

$$\hat{H}^2 = \begin{pmatrix} mc^2 & 2cp_z + imc\tilde{\omega}\bar{z} \\ 2cp_{\bar{z}} - imc\tilde{\omega}z & -mc^2 \end{pmatrix}. \quad (3.6)$$

We note that the 2+1 DMO with angular frequency ω in the presence of the magnetic field maps into 2+1 DMO where the angular frequency ω changes to $\tilde{\omega} = \omega + \frac{\omega_c}{2}$, which means the magnetic field decreases the angular frequency by half of the cyclotron frequency of this system.

In order to find the solution, we define the following creation and annihilation operators:

$$\hat{a} = \frac{1}{\sqrt{m\tilde{\omega}\hbar}}p_{\bar{z}} - \frac{i}{2}\sqrt{\frac{m\tilde{\omega}}{\hbar}}z, \quad (3.7)$$

$$\hat{a}^\dagger = \frac{1}{\sqrt{m\tilde{\omega}\hbar}}p_z + \frac{i}{2}\sqrt{\frac{m\tilde{\omega}}{\hbar}}\bar{z}, \quad (3.8)$$

where $[\hat{a}, \hat{a}^\dagger] = 1, [\hat{a}, \hat{a}] = 0 = [\hat{a}^\dagger, \hat{a}^\dagger]$.

Now, we can write the Hamiltonian \hat{H}^2 (3.6) in terms of the creation and annihilation operators as follows:

$$\hat{H}^2 = \eta(\hat{a}^\dagger \hat{\sigma}_+ + \hat{a} \hat{\sigma}_-) + mc^2 \hat{\sigma}_z, \quad (3.9)$$

where $\eta = 2\sqrt{mc^2 \tilde{\omega} \hbar}$. This equation represents the Hamiltonian of the Anti-JCM in quantum optics.

In the presence of an external isospin field Φ , the dynamics of the total system is given by the Hamiltonian

$$\tilde{H} = \hat{H}^2 + \Phi, \quad (3.10)$$

where \hat{H}^2 is given by Eq. (3.9) and Φ is the hermitean operator. It takes the following form [25]

$$\Phi = (A + \hat{\sigma}_z B)(\hat{a} \hat{\sigma}_+ + \hat{a}^\dagger \hat{\sigma}_- + \gamma \hat{\sigma}_z), \quad (3.11)$$

where $\hat{\sigma}$'s are the vectors of Pauli matrices, they have the same commutation relations as $\hat{\sigma}$'s, so, the corresponding ladder operators are defined by

$$\hat{\sigma}_\pm = \frac{1}{2}(\hat{\sigma}_x \pm i\hat{\sigma}_y). \quad (3.12)$$

We use the simplest form of Φ (i.e.linear) as

$$\Phi = \chi(\hat{a} \hat{\sigma}_+ + \hat{a}^\dagger \hat{\sigma}_-) + \gamma \hat{\sigma}_z. \quad (3.13)$$

\tilde{H} can be described in quantum optics as GJCM, where \hat{a} is the annihilation operator of the cavity field and each isospin with an atom, while η and χ can be described as the coupling of each atom to the cavity isospin and mc^2 and γ are described as the detuning of each transition level with the cavity mode frequency. This model can be seen as a linear combination of the two JCM. This model may be considered general than the model in [22], where in our model we take into account the influence of the magnetic field, which lead to map this model into the GJCM.

In order to solve this system (3.10), we use the Heisenberg equation of motion to deduce the constant of motion as follow

$$I = \hat{n} + \frac{1}{2}(\dot{\sigma}_z - \hat{\sigma}_z), \quad (3.14)$$

with $\hat{n} = \hat{a}^\dagger \hat{a}$.

4 The analytical solution

This section is devoted to derive the wave function $|\psi(t)\rangle$ and the reduced density operators. We assume the two particles (the particle in DMO and the isospin field) and the electromagnetic field are initially prepared in ground states and coherent state respectively. In this case, the wave function of this system at $t = 0$ can be written as

$$|\psi(0)\rangle = |-\rangle_{Ds} \otimes |-\rangle_{Is} \otimes |\alpha\rangle_F, \quad (4.1)$$

where

$$|\alpha\rangle = \sum_{n=0}^{\infty} q_n |n\rangle, \quad (4.2)$$

with

$$q_n = \exp\left(\frac{-|\alpha|^2}{2}\right) \frac{\alpha^n}{\sqrt{n!}}, \alpha \in \mathbb{C}. \quad (4.3)$$

By using the constant of motion Eq. (3.14), the wave function $|\psi(t)\rangle$ takes the following form at $t > 0$

$$\begin{aligned} |\psi(t)\rangle = & \sum_{n=0}^{\infty} (B_1(n, t) |-\dot{-}, n+2\rangle + B_2(n, t) |+\dot{-}, n+3\rangle \\ & + B_3(n, t) |-\dot{+}, n+1\rangle + B_4(n, t) |+\dot{+}, n+2\rangle). \end{aligned} \quad (4.4)$$

We obtain the coefficients $B_j(n, t)$, ($j = 1, 2, 3, 4$) by solving the Schrödinger equation. Therefore, we have the following system of differential equations for the $B_j(n, t)$ coefficients

$$i\hbar \dot{B}_1(n, t) = a(n)B_2(n, t) + d(n)B_3(n, t) - 2\Omega B_1(n, t), \quad (4.5)$$

$$i\hbar\dot{B}_2(n, t) = a(n)B_1(n, t) + c(n)B_4(n, t), \quad (4.6)$$

$$i\hbar\dot{B}_3(n, t) = b(n)B_4(n, t) + d(n)B_1(n, t), \quad (4.7)$$

$$i\hbar\dot{B}_4(n, t) = b(n)B_3(n, t) + c(n)B_2(n, t) + 2\Omega B_1(n, t), \quad (4.8)$$

where

$$a(n) = \lambda_1\sqrt{n+3}, b(n) = a(n-1), \quad (4.9)$$

$$c(n) = \lambda_2\sqrt{n+3}, d(n) = c(n-1), \quad (4.10)$$

$$mc^2 = \gamma = \Omega, \quad (4.11)$$

with

$$\lambda_1 = \frac{2\sqrt{1+\xi}}{\eta}, \lambda_2 = \frac{\chi}{\eta\sqrt{mc^2\omega}} \text{ and } \xi = \frac{eB}{2mc\omega}.$$

We take $c = 1 = \hbar$. The time-dependent coefficients $B_j(n, t)$, ($j = 1, 2, 3, 4$) are obtained, by solving the above differential equations (4.5-4.8). With the wave function $|\psi(t)\rangle$ calculated, then calculations for any property related to the particles or the field can be performed.

The reduced density operator of the isospin field $\dot{\rho}(t)$ can be obtained as following

$$\begin{aligned} \dot{\rho}(t) &= Tr_F Tr_{DO} |\psi(t)\rangle \langle \psi(t)| \\ &= \dot{\rho}_{ee}(t) |\dot{+}\rangle \langle \dot{+}| + \dot{\rho}_{gg}(t) |\dot{-}\rangle \langle \dot{-}| + \\ &\quad \dot{\rho}_{eg}(t) |\dot{+}\rangle \langle \dot{-}| + \dot{\rho}_{ge}(t) |\dot{-}\rangle \langle \dot{+}|, \end{aligned} \quad (4.12)$$

where

$$\dot{\rho}_{ee}(t) = \sum_{n=0}^{\infty} (|B_3(n, t)|^2 + |B_4(n, t)|^2), \quad (4.13)$$

$$\dot{\rho}_{gg}(t) = \sum_{n=0}^{\infty} (|B_1(n, t)|^2 + |B_2(n, t)|^2), \quad (4.14)$$

$$\dot{\rho}_{eg}(t) = \sum_{n=0}^{\infty} (B_3(n+1, t)B_1^*(n, t) + B_4(n+1, t)B_2^*(n, t)) = \dot{\rho}_{ge}^*(t). \quad (4.15)$$

Also, to obtain the reduced density matrix of the two particles, we trace over the oscillator degree of freedom

$$\begin{aligned}\rho(t) &= \text{Tr}_F |\psi(t)\rangle \langle \psi(t)| \\ &= \begin{pmatrix} \rho_{11}(t) & \rho_{12}(t) & \rho_{13}(t) & \rho_{14}(t) \\ \rho_{21}(t) & \rho_{22}(t) & \rho_{23}(t) & \rho_{24}(t) \\ \rho_{31}(t) & \rho_{32} & \rho_{33}(t) & \rho_{34}(t) \\ \rho_{41}(t) & \rho_{42} & \rho_{43}(t) & \rho_{44}(t) \end{pmatrix},\end{aligned}\tag{4.16}$$

where

$$\begin{aligned}\rho_{11}(t) &= \sum_{n=0}^{\infty} |B_1(n, t)|^2, \rho_{22}(t) = \sum_{n=0}^{\infty} |B_2(n, t)|^2, \\ \rho_{33}(t) &= \sum_{n=0}^{\infty} |B_3(n, t)|^2, \rho_{44}(t) = \sum_{n=0}^{\infty} |B_4(n, t)|^2, \\ \rho_{12}(t) &= \sum_{n=0}^{\infty} B_1(n+1, t) B_2^*(n, t) = \rho_{21}^*(t), \\ \rho_{13}(t) &= \sum_{n=0}^{\infty} B_1(n, t) B_3^*(n+1, t) = \rho_{31}^*(t), \\ \rho_{14}(t) &= \sum_{n=0}^{\infty} B_1(n, t) B_4^*(n, t) = \rho_{41}^*(t), \\ \rho_{23}(t) &= \sum_{n=0}^{\infty} B_2(n, t) B_3^*(n+2, t) = \rho_{32}^*(t), \\ \rho_{34}(t) &= \sum_{n=0}^{\infty} B_3(n+1, t) B_4^*(n, t) = \rho_{43}^*(t).\end{aligned}\tag{4.17}$$

With these operators given, different statistical properties of this system can be studied.

5 Non-classical properties

In this section, we discuss some statistical properties of the present system, where we concentrate on the influence of the strength of the magnetic field and the coupling

constant parameter of the isospin field on the behaviour of the entanglement and the population inversion and the correlation function.

5.1 Entanglement

In this subsection we study the entanglement between the DMO and the isospin field through the von Neumann entropy. In quantum optics the von Neumann entropy has been used to study the dynamic characteristics of a two-level atom interacting with light [26]. It is noted that this measure is a useful physical quantity for measuring the degree of entanglement in a pure state.

The von Neumann entropy is defined in quantum mechanics as [22, 27],

$$S(t) = -\lambda_-(t) \ln \lambda_-(t) - \lambda_+(t) \ln \lambda_+(t), \quad (5.1)$$

where $\lambda_{\pm}(t)$ are the eigenvalues of the reduced density matrix $\dot{\rho}(t)$ Eqs. (4.12-4.15). They can be easily evaluated through the following form:

$$\lambda_{\pm}(t) = \frac{1}{2} \pm \frac{1}{2} \sqrt{\langle \hat{\sigma}_x(t) \rangle^2 + \langle \hat{\sigma}_y(t) \rangle^2 + \langle \hat{\sigma}_z(t) \rangle^2}, \quad (5.2)$$

where

$$\langle \hat{\sigma}_x(t) \rangle = 2\Re[\dot{\rho}_{eg}(t)], \quad (5.3)$$

$$\langle \hat{\sigma}_y(t) \rangle = 2\Im[\dot{\rho}_{eg}(t)], \quad (5.4)$$

$$\langle \hat{\sigma}_z(t) \rangle = \dot{\rho}_{ee}(t) - \dot{\rho}_{gg}(t). \quad (5.5)$$

In Figs. (1,2), we display the effect of the strength of the magnetic field and the coupling parameter of the isospin field on the evolution of the von Neumann entropy against the scaled time λt , where $\lambda = \eta\sqrt{mc^2\omega}$, when the atoms in ground state initially and the field be prepared initially in the coherent state. The value of the intensity of the initial coherent parameter has been fixed as $\alpha = 3$ and the detuning parameter has been fixed as $\Omega = 0.2\lambda$.

We note that $S(t)$ starts from zero, then it followed by a sequence of fluctuations in the oscillation. This means that this system begins by disentangled state (at

$\lambda t = 0$) then it develops to a mixed state (at $\lambda t > 0$) and never reaches to the pure state again.

In Fig. (1), the effect of the strength of the magnetic field (λ_1) appear clearly where there is a sudden decrease in the value of $S(t)$ as λt ranges from 20 to 40, see Fig. (1a). Also an extra minimum (decrease of $S(t)$) occurs as λ_1 increases at the same period Fig. (1c,1d), also the entanglement increases for a longer period ($\lambda t > 40$). By increasing λ_1 , $S(t)$ oscillates near the maximum value of $(\ln 2)$.

Fig. (2) shows the effect of the coupling parameter of the isospin field (λ_2) on the entanglement, we observe that by increasing the value of this parameter, the value of entanglement increases also the number of the fluctuation increases.

We may conclude that to obtain strong entanglement between the isospin field and the Dirac oscillator, we increase the value of λ_1 or λ_2 .

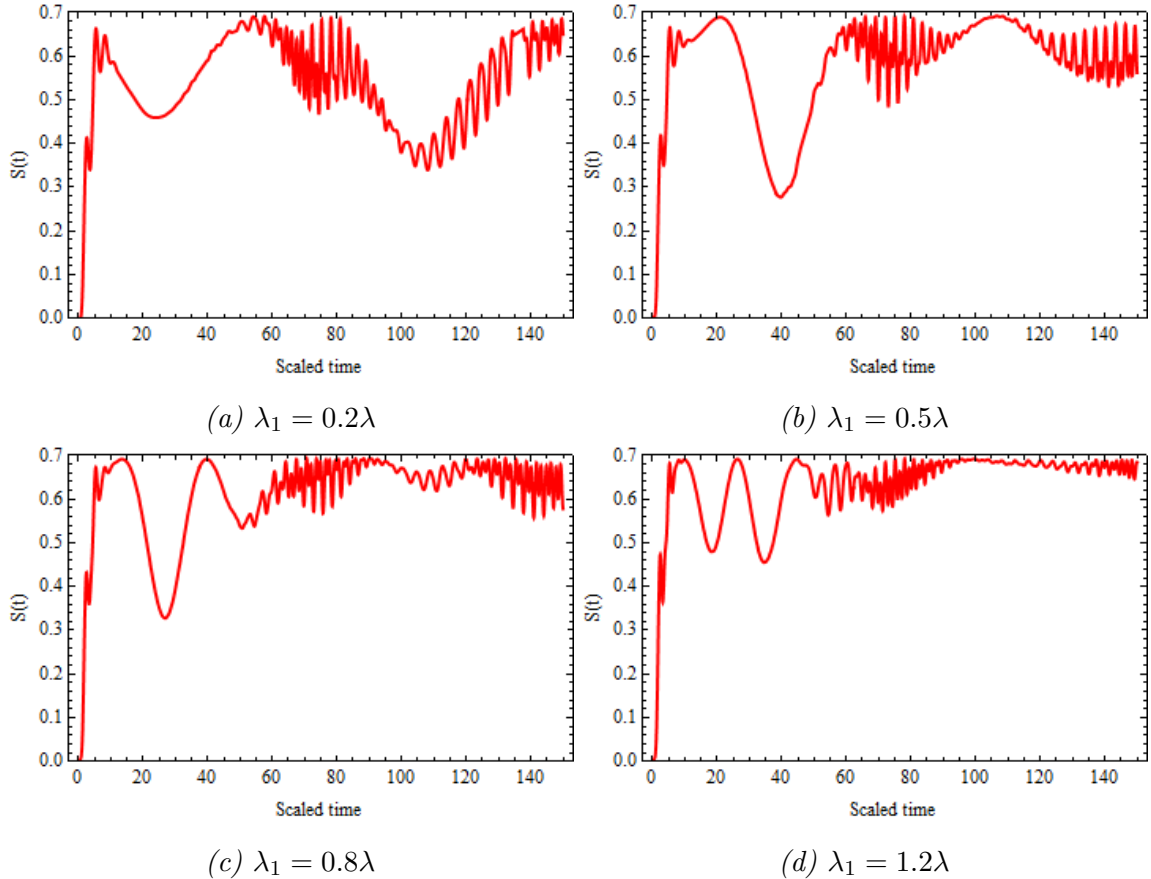


Figure 1: The von Neumann entropy is plotted as a function of λt with $\Omega = 0.2\lambda$ and $\lambda_2 = 0.3\lambda$.

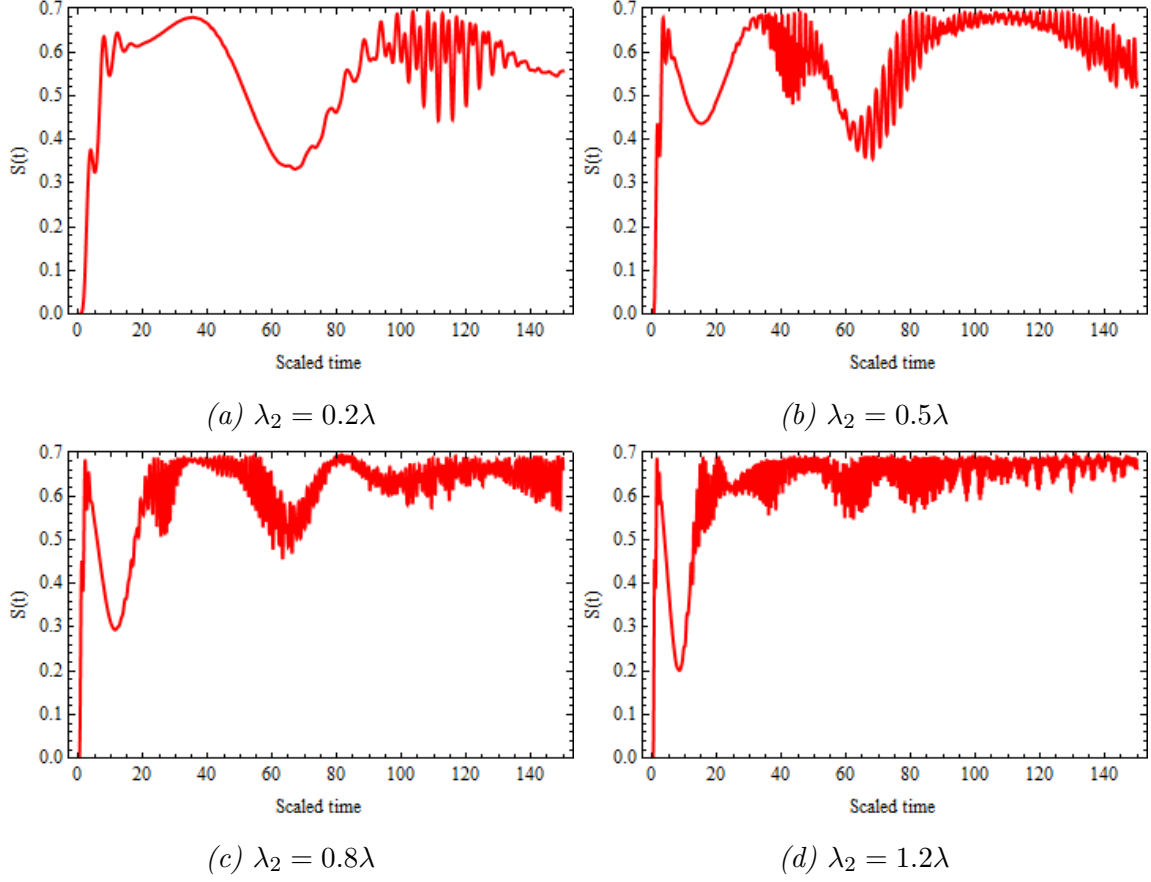


Figure 2: The von Neumann entropy is plotted as a function of λt with $\Omega = 0.2\lambda$ and $\lambda_1 = 0.3\lambda$.

5.2 Concurrence

In this subsection, we use the concurrence to measure the entanglement between the two particles. It ensures the scale between 0 for a separable (disentangled) state and $\sqrt{2(N-1)/N}$ for the maximally entangled state. The concurrence may be written in the following form [28, 29]:

$$C(t) = \sqrt{2 \sum_{i,j=1,2,3,4} (\rho_{ii}(t)\rho_{jj}(t) - \rho_{ij}(t)\rho_{ji}(t)), i \neq j},$$

where $\rho_{ii}(t)$, $\rho_{jj}(t)$, $\rho_{ji}(t)$ and $\rho_{ij}(t)$ are given by (4.17).

In Figs. (3, 4), we plot the evolution of concurrence $C(t)$ versus the scaled time λt , in order to see the effect of λ_1 and λ_2 on the degree of the entanglement between the two particles (the isospin field and the particle in DMO). We use the same initial

parameters as the previous figures.

It is noted that $C(t)$ starts from zero, then it is followed by a sequence of fluctuations between *zero* and 1.2, this means that the entanglement between the two particles can not be performed before the interaction is switched on. To visualize the effect of λ_1 , see Fig. (3) where we take different values of λ_1 . It is observed that for a large effect of λ_1 , the entanglement increases after a short time from the start, and the number of rapid fluctuations increases, see Figs. (3c, 3d).

The same behaviour appears in Fig. (4), where we use different values of λ_2 . We can say that the effect of λ_1 on the degree of the entanglement between the two particles is similar to the effect of λ_2 , where, by increasing the value of any of these parameters, the degree of entanglement increases.

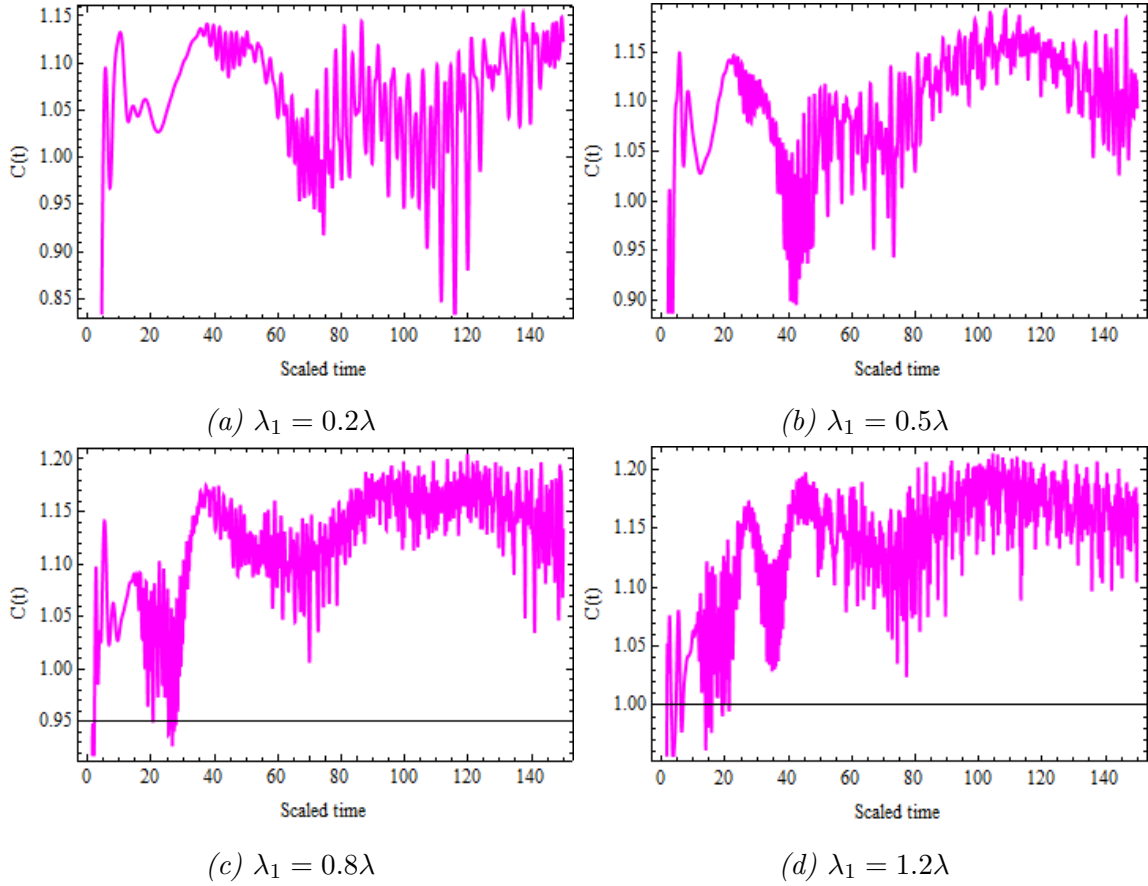


Figure 3: The concurrence is plotted as a function of λt . The parameters are similar to 1.

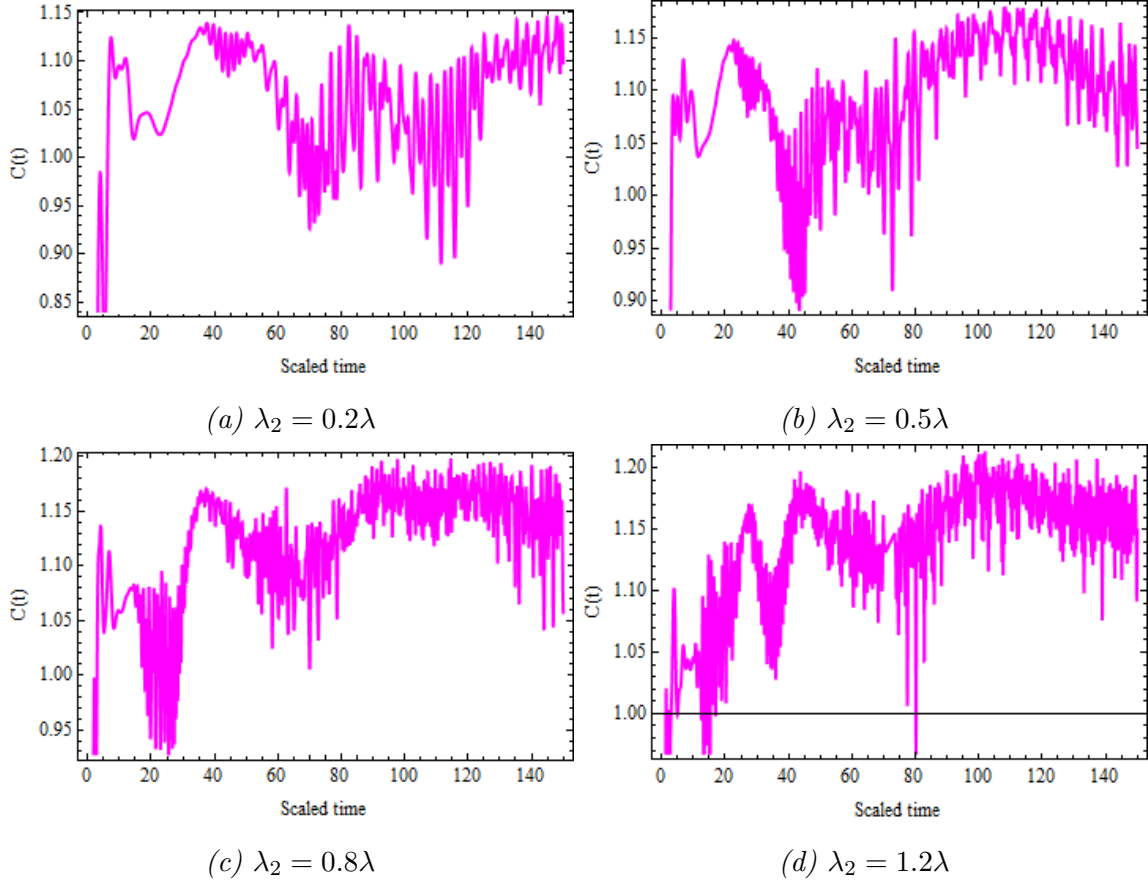


Figure 4: The concurrence is plotted as a function of λt . The parameters are similar to 2.

5.3 The population inversion

The population inversion gives us information about the behaviour of the particle during the interaction period, which determines when this particle reaches its maximal state and leads one to observe when this particle is in its excited or ground state or in a superposition state. From mathematical point of view the population inversion is the expectation value of the operator $\hat{\sigma}_z$, thus we have

$$W(t) = \dot{\rho}_{ee}(t) - \dot{\rho}_{gg}(t). \quad (5.6)$$

We display the evolution of the population inversion of the isospin field for different values of λ_1 in Fig. (5) and we use different values of λ_2 in Fig. (6). We use the same initial parameters as the previous figures. We note that the collapses and revivals phenomenon is very obvious in all figures, the function $W(t)$ is symmetric around $W(t) = 0$ and the population inversion oscillates between (-1) and $(+1)$.

We observe that the strength of the magnetic field does not affect strongly on the behaviour of the isospin field, see Fig. (5). We see the opposite in Fig. (6), where by increasing the values of λ_2 , the collapse period decreases and the oscillation increases during the revival period, see Fig. (6b). By taking large value of λ_2 , the oscillation increases rapidly and the collapses and revivals phenomenon do not appear as clearly as before due its interference between the patterns, see Figs. (6c, 6d).

We can say that in order to study the behaviour of the isospin field and show the collapses and revivals phenomenon clearly in this system, we simply increase the value of λ_2 .

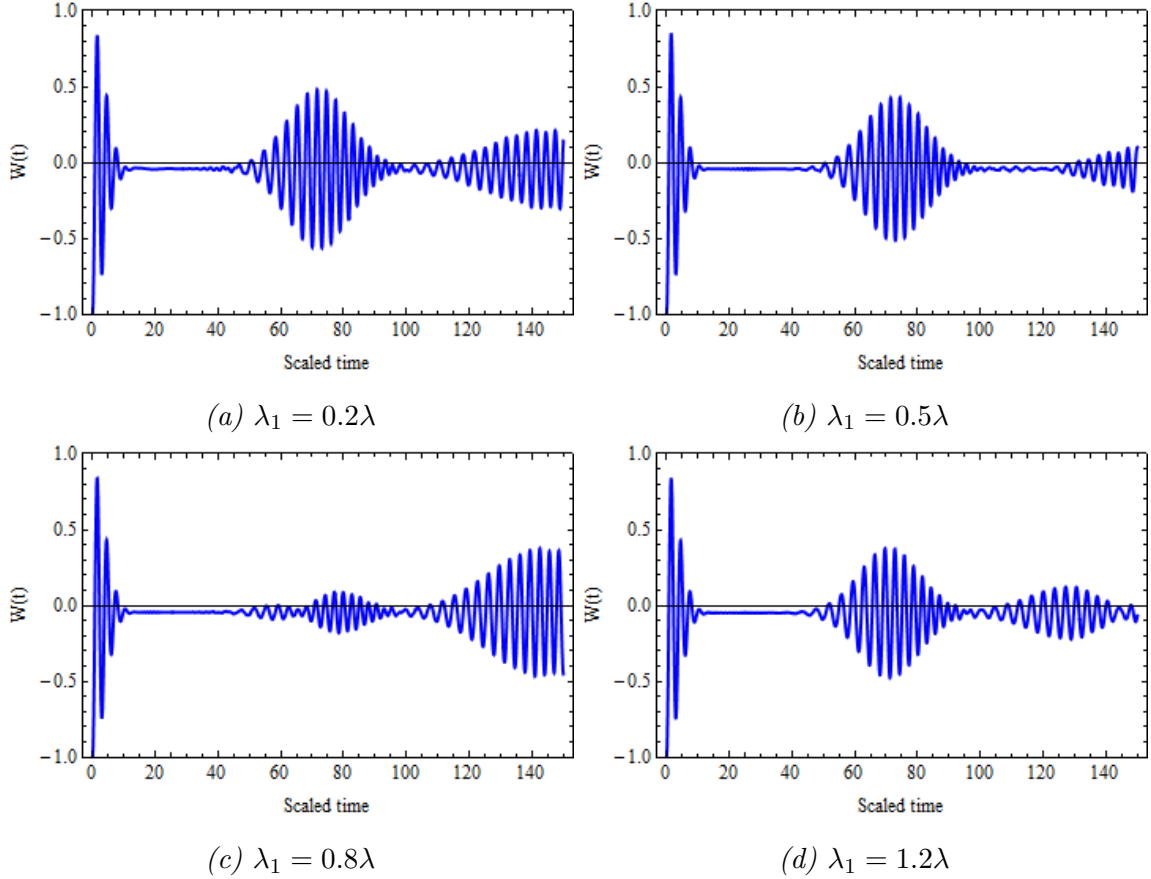


Figure 5: The population inversion of the isospin field is plotted as a function of λt . The parameters are similar to 1.

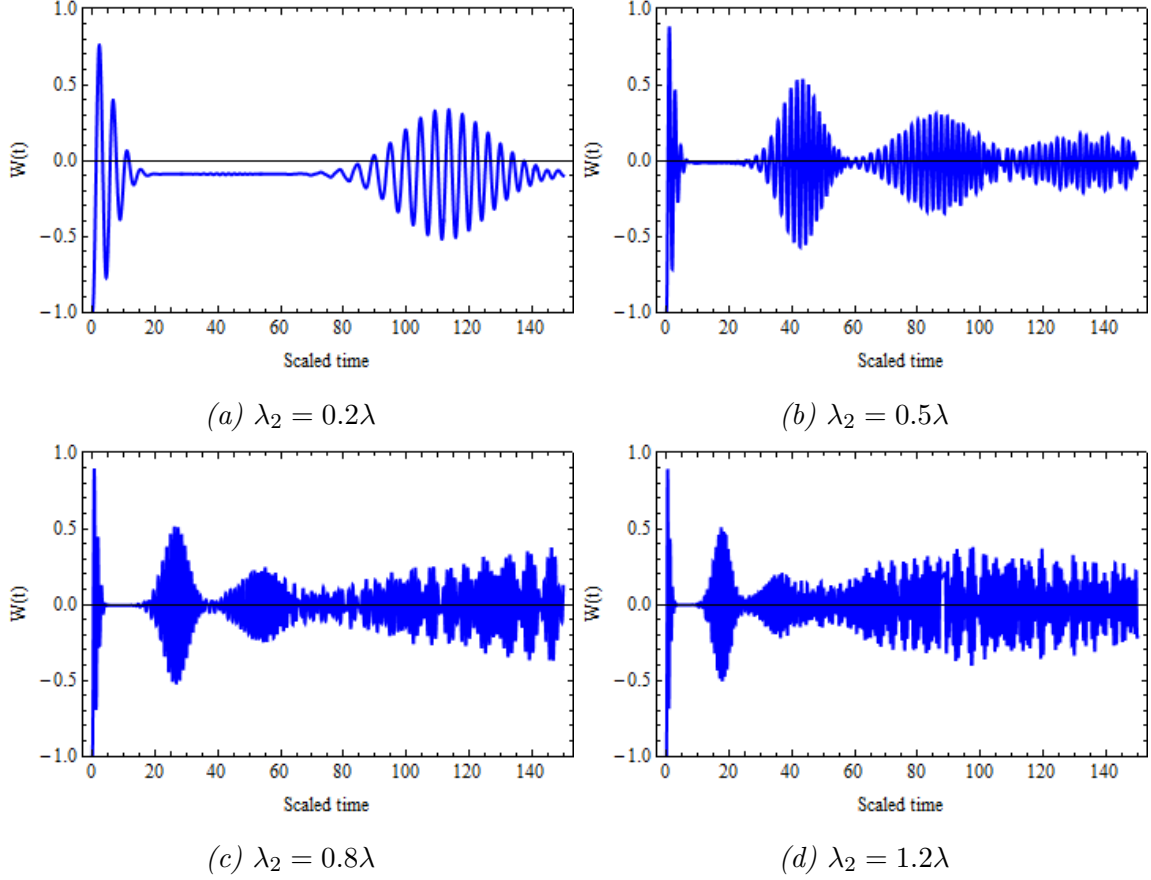


Figure 6: The population inversion of the isospin field is plotted as a function of λt . The parameters are similar to 2.

5.4 The Second-order coherence

No doubt the examination of the second-order correlation function leads to better understanding for the non-classical behaviour of the system. For this reason, we devote the present subsection to discuss the behaviour of the correlation function for the present system. The correlation function is usually used to discuss the sub-Poissonian and super-Poissonian behaviour of the photon distribution. By using this function, we can distinguish between classical and non-classical behaviour of the system. The normalized second-order correlation function is defined by [24]

$$g^{(2)}(t) = \frac{\langle \hat{a}^{\dagger 2} \hat{a}^2 \rangle}{\langle \hat{a}^{\dagger} \hat{a} \rangle^2}. \quad (5.7)$$

A light field has a sub-Poissonian distribution if $g^{(2)}(t) < 1$, which is a non-classical effect and means that the probability of detecting an incident pair of pho-

tons is less than it would be for a coherent field described by the Poissonian distribution. On the other hand, light has super-Poissonian distribution if $g^{(2)}(t) > 1$, which is a classical effect, and a Poissonian distribution of photon (standard for the coherent state) if $g^{(2)}(t) = 1$. In the meantime, the system displays thermal statistics when $g^{(2)}(t) = 2$ and super-thermal for $g^{(2)}(t) > 2$. In order to discuss the distribution of this system, we calculate the expectation value of the quantities $\langle \hat{a}^{\dagger 2} \hat{a}^2 \rangle$ and $\langle \hat{a}^{\dagger} \hat{a} \rangle^2$

$$\begin{aligned} \langle \hat{a}^{\dagger 2} \hat{a}^2 \rangle &= \langle \hat{n}(\hat{n} - 1) \rangle = \\ &\sum_{n=0}^{\infty} [(n+1)(n+2) |B_1(n, t)|^2 + (n+2)(n+3) |B_2(n, t)|^2 \\ &+ n(n+1) |B_3(n, t)|^2 + (n+1)(n+2) |B_4(n, t)|^2]. \end{aligned} \quad (5.8)$$

$$\begin{aligned} \langle \hat{a}^{\dagger} \hat{a} \rangle^2 &= \langle \hat{n} \rangle^2 = \\ &\left(\sum_{n=0}^{\infty} [(n+2) |B_1(n, t)|^2 + (n+3) |B_2(n, t)|^2 + \right. \\ &\left. (n+1) |B_3(n, t)|^2 + (n+2) |B_4(n, t)|^2] \right)^2 \end{aligned} \quad (5.9)$$

By using Eqs. (5.7)-(5.9) we can easily get $g^{(2)}(t)$.

Now, we discuss the numerical calculations of the second-order correlation function $g^{(2)}(t)$ in Figs. (7, 8). It is observed that the oscillation base line is oscillating around 0.987 and never reaches 1 after $\lambda t > 0$, which means, the system is exhibiting sub-Poissonian distribution, but the distribution is Poissonian at the beginning. Also, by increasing values of λ_1 or λ_2 , the oscillation is squeezed and still sub-Poissonian.

6 Conclusion

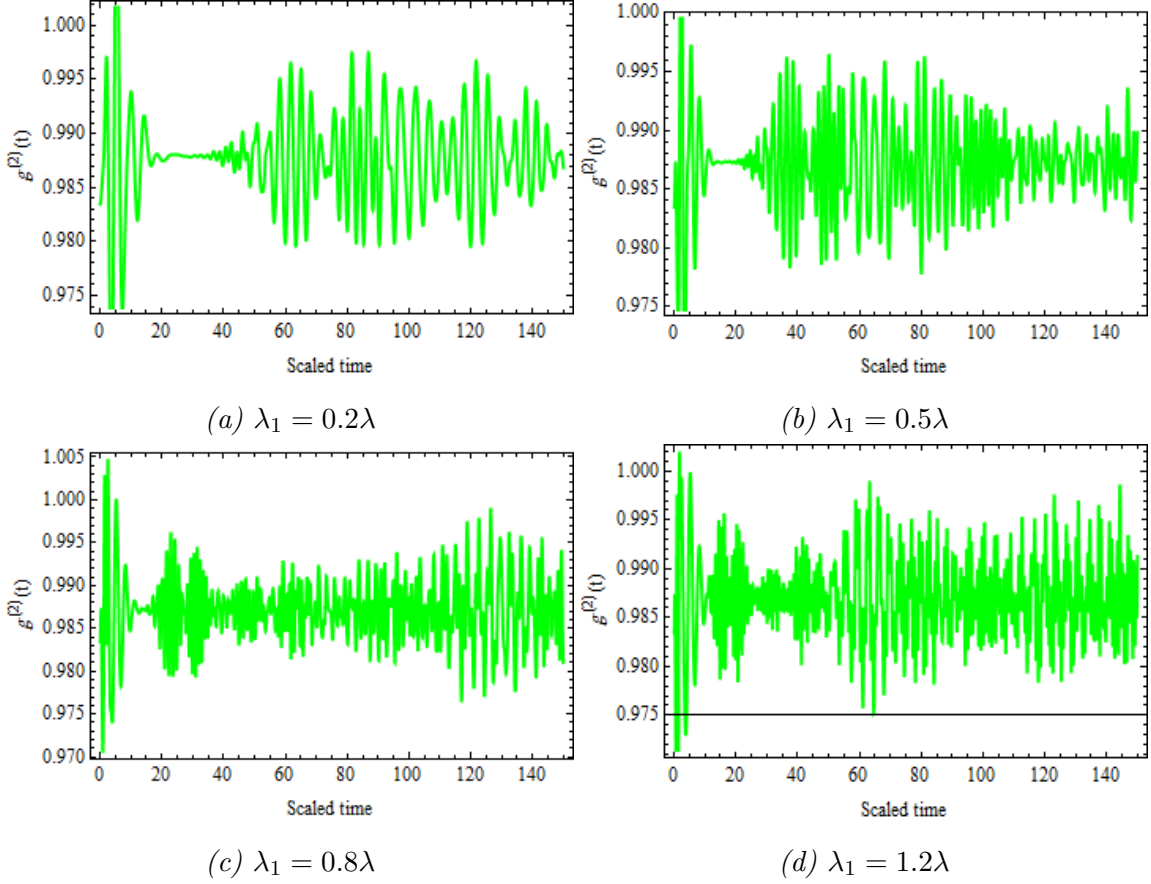


Figure 7: The second order correlation is plotted as a function of λt with . The parameters are similar to 1.

We have studied how the 2+1 DMO coupled to an external isospin field in an external magnetic field is mapped into the GJCM. Also, we studied the effect of the strength of the magnetic field (λ_1) and the coupling parameter of the isospin field (λ_2) on the entanglement, the population inversion and the second-order correlation function. We have used the coherent state as the initial state and fixed the value of the initial coherent parameter as $\alpha = 3$. The model is considered more general than the model obtained in [22], where we added to the 2+1 DMO an external magnetic field which is neglected in [22]. Also, this model is more general than the model obtained in [19], where we use an external isospin field and study some statistical properties of the system.

We would like to clarify that the strength of the magnetic field and the coupling parameter have clear effects on the entanglement between the isospin field and the Dirac oscillator, also, between the two particles.

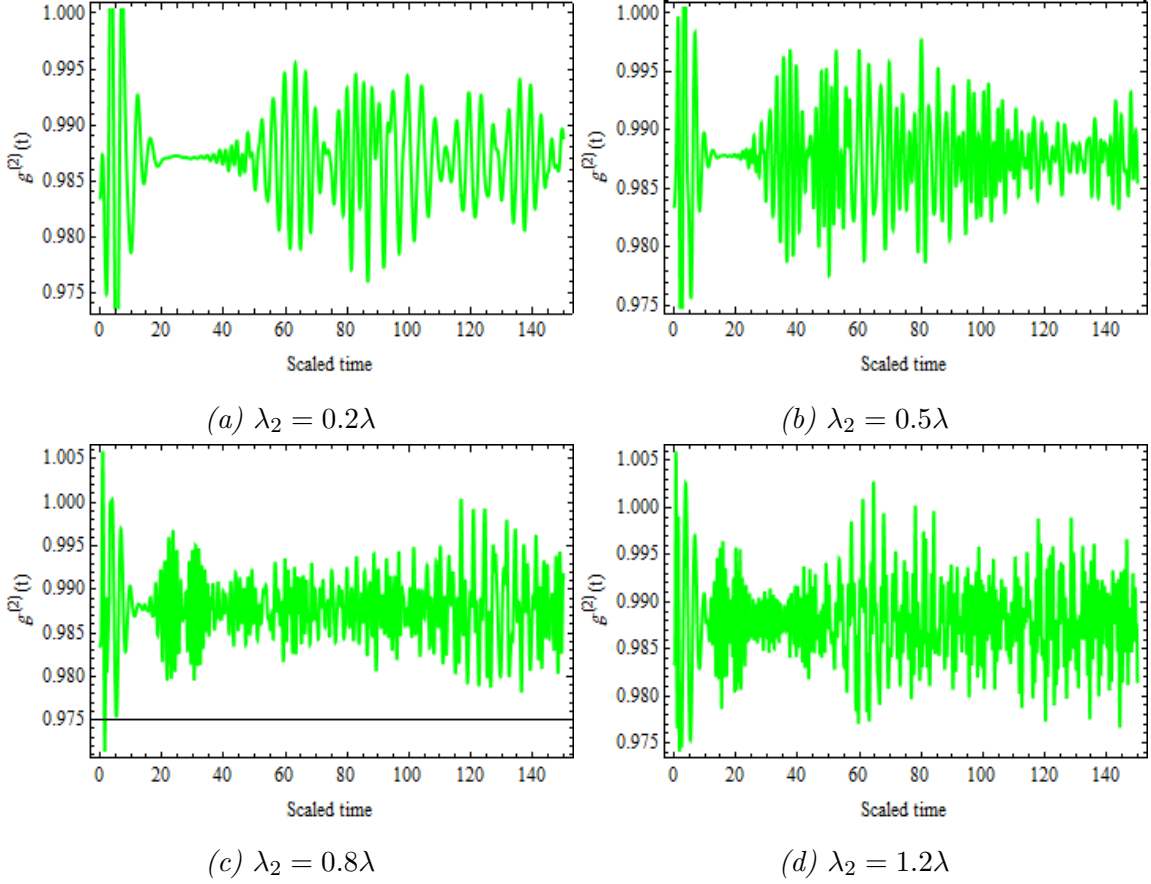


Figure 8: The second order correlation is plotted as a function of λt . The parameters are similar to 2.

The 2+1 DMO and the isospin field are separated at $\lambda t = 0$ and they are in a mixed state and never reach to the pure state again for any time $\lambda t > 0$.

By increasing the value of λ_1 or the value of λ_2 , we can obtain strong entanglement between the isospin field and the Dirac oscillator, see Figs. (1, 2), also the degree of entanglement between the two particles increases in a similar way, see Figs. (3, 4).

The behaviour of the isospin field and the collapses and revivals phenomenon are shown clearly, by simply increasing the value of λ_2 , see Fig. (6).

The system is exhibiting sub-Poissonian distribution for any time $\lambda t > 0$.

So, this paper shows how important is the link between quantum optics and quantum relativistic, where this link helps to study some of the statistical properties of the 2+1 DMO coupled to an external isospin field in an external magnetic field. These statistical properties have not been studied without this link.

References

- [1] E. T. Jaynes and F. W. Cummings, Proc. IEEE **51**, 89 (1963).
- [2] S. Haroche and J. M. Raimond, Exploring the Quantum: Atoms, Cavities and Photons (Oxford University Press, Oxford, 2007).
- [3] J. H. Eberly, N. B. Narozhny and J. J. S. -Mondragon, Phys. Rev. Lett. **44**, 1323 (1980).
- [4] N. B. Narozhny, J. J. S. -Mondragon and J.H. Eberly, Phys. Rev. A **23**, 236 (1981).
- [5] M. A. Nielsen and I. L. Chuang, Quantum Computation and Quantum Information (Cambridge: Cambridge University Press, 2010).
- [6] D. Ito, K. Mori, and E. Carrieri, Nuovo Cimento A **51** , 119 (1967).
- [7] P. A. Cook, Lett. Al Nuovo Cimento **1**, 419 (1971).
- [8] M. Moshinsky and A. Szczepaniak, J. Phys. A **22**, 817 (1989).
- [9] D. Ojeda-Guillén, R. D. Mota, and V. D. Granados, J. Math. Phys. **57**, 062104 (2016).
- [10] F. M. Toyama, Y. Nogami, and F. A. B. Coutinho, J. Phys. A: Math. Gen. **30**, 2585 (1997).
- [11] R. Szmytkowski and M. Gruchowski, J. Phys. A: Math. Gen. **34**, 4991 (2001).
- [12] N. Ferkous and A. Bounames, Phys. Lett A **325**, 21 (2004).
- [13] R. de L. Rodrigues, Phys. Lett. A **372**, 2587 (2008).
- [14] A. Bermudez, M. A. M. Delgado and A. Luis, Phys. Rev. A **77**, 063815 (2008).
- [15] A. Bermudez, M. A. Martin-Delgado, and E. Solano, Phys. Rev. A **76**, 041801 (2007).

- [16] E. Sadurni, J. M. Torres, and T. H. Seligman, J. Phys. A: Math. Theor. **43**, 285204 (2010).
- [17] A. Bermudez, M. A. Martin-Delgado and E. Solano, Phys. Rev. A **76**, 041801 (2007).
- [18] J. Benítez, R. P. M. Y. Romero, H. N. Núñez-Yépez and A. L. Salas-Brito, Phys. Rev. Lett. **64**, 1643 (1990); Erratum, Phys. Rev. Lett. **65**, 2085 (1990).
- [19] B. P. Mandal and S. Verma, Phys. Lett. A **374**, 1021 (2010).
- [20] A. Bermudez, M. A. Martin-Delgado and E. Solano, Phys. Rev. A **76**, 041801 (2007).
- [21] J. M. Torres, E. Sadurmi and T. H. Seligman, AI P Conference Proceedings **1323**, 301 (2010).
- [22] A. S.-F. Obada, M. M. A. Ahmed, M. Abu-Shady and H. F. Habeba, J RUSS LASER RES **43**, 132(2019).
- [23] W. Greiner, "Relativistic Quantum Mechanics: Wave Equations", (Springer, Berlin, 2000).
- [24] M. O. Scully and M. S. Zubairy, "Quantum Optics", (Cambridge University Press, 1997).
- [25] E. Sadurni, J. M. Torres and T. H. Seligman, J. Phys. A **43**, 285204 (2010).
- [26] M. S. Abdalla, M. M. A. Ahmed and A. -S. F. Obada, Laser Phys. **25**, 065204 (2015) .
- [27] J. von Neumann, "Mathematical Foundations of Quantum Mechanics", (Princeton University Press, Princeton 1955).
- [28] F. Minter, M. Kus and A. Buchleitner, Phys. Rev. Lett. **95**, 160 (2005).
- [29] M. Abdel-Aty, Prog Quantum Electron **31**,1 (2007).